minerals

MDPI

Article

Removal of Pyrrhotite from High-Sulphur Tailings Utilising Non-Oxidative H_2SO_4 Leaching

Jarno Mäkinen [1,*], Grzegorz Pietek [1], Ville Miettinen [2], Mohammad Khoshkhoo [3], Jan-Eric Sundkvist [3] and Päivi Kinnunen [1]

[1] VTT Technical Research Centre of Finland Ltd., Visiokatu 4, 33101 Tampere, Finland
[2] Finnish Minerals Group, Keskuskatu 5 B, 00101 Helsinki, Finland
[3] Boliden Mineral AB, Fällforsvägen 4, SE-936 81 Boliden, Sweden
* Correspondence: jarno.makinen@vtt.fi

Abstract: Tailings are a residual material stream produced in the mineral processing of ores. They may contain a major sulphide content that increases the risk of acid rock drainage (ARD) but may also host valuable metals. Tank bioleaching is a technically viable method to treat sulphide tailings. However, a significant pyrrhotite content may cause increased acid and oxidant consumption and result in longer retention times in a bioleaching process. In this work, non-oxidative H_2SO_4 leaching of pyrrhotite is studied for high-sulphur tailings, both as a pre-treatment method and to consider the recovery possibilities of Fe and S. Continuous mode validation tests, conducted at 90 °C, pH 1.0 and 106 min retention time, resulted in a complete pyrrhotite dissolution with 427 kg/t acid consumption (as 95% H_2SO_4). Unwanted dissolution of Ni and Zn was taking place with a leaching yield of 21.5% and 13.5%, respectively, while Co and Cu dissolution was negligible. The continuous mode tests signalled that by shortening the retention time, Ni dissolution could be dramatically decreased. The non-oxidative pyrrhotite leaching produced a H_2S-rich gas stream, which could be utilised in later metals' recovery processes after bioleaching to precipitate (CoNi)S, ZnS and CuS products. The non-oxidative pyrrhotite leaching also produced a $FeSO_4$ solution, with approximately 20 g/L of Fe.

Keywords: pyrrhotite; pyrite; cobalt; nickel; leaching

Citation: Mäkinen, J.; Pietek, G.; Miettinen, V.; Khoshkhoo, M.; Sundkvist, J.-E.; Kinnunen, P. Removal of Pyrrhotite from High-Sulphur Tailings Utilising Non-Oxidative H_2SO_4 Leaching. *Minerals* **2022**, *12*, 1610. https://doi.org/10.3390/min12121610

Academic Editor: Jean-François Blais

Received: 26 October 2022
Accepted: 6 December 2022
Published: 14 December 2022

1. Introduction

In the mineral processing of sulphide ores, flotation technology is widely used to separate and concentrate targeted valuable minerals. During this action, a residual solid, called tailings, is produced and rejected into tailing ponds [1,2]. This material is a mixture of fine particle-sized gangue minerals and process water. Depending on the characteristics of the ore and flotation process, tailings may contain reactive sulphides which increase the risk of acid rock drainage (ARD) in disposal sites [3,4]. In addition, sulphide minerals in tailings may host valuable metals that are currently lost [3]. If feasible, an additional flotation step may be applied to separate remaining sulphides (typically pyrite FeS_2 and/or pyrrhotite $Fe_{0.83-1}S$) from non-sulphidic gangue material, to produce "high-sulphur (HS) tailings" or "sulphur concentrate". This enables better management of the ARD risk and later recovery of valuable metals from historic ponds.

Some HS tailings and related side-streams have contained such a high concentration of valuable metals that their additional treatment has been economically possible. For example, Kasese Cobalt Company (KCC) in Uganda treated HS tailings for Co recovery by utilising tank bioleaching technology [5]. Similarly, Mondo Minerals in Finland utilised tank bioleaching of sulphur concentrate for Ni recovery [6]. Even though these plants utilised a similar leaching technology, their behaviour was different: the KCC leaching circuit required $CaCO_3$ to neutralise the excess acidity during the leaching, while the Mondo Minerals plant faced a net acid consumption and thus external H_2SO_4 addition was

required. The explanation for this difference is likely the different mineralogy, as the KCC material was extremely rich in pyrite, while the Mondo Minerals feed contained pyrrhotite and pentlandite [5,6].

Pyrrhotite is a highly reactive mineral that consumes plenty of acid and oxidant in leaching circuits, as shown in Equations (1)–(3) [7–10].

$$Fe_7S_8 + 7H_2SO_4 \rightarrow 7FeSO_4 + 7H_2S + S^0 \quad (1)$$

$$Fe_7S_8 + 7H_2SO_4 + 3.5O_2 \rightarrow 7FeSO_4 + 7H_2O + 8S^0 \quad (2)$$

$$Fe_7S_8 + 7Fe_2(SO_4)_3 \rightarrow 21FeSO_4 + 8S^0 \quad (3)$$

Generally, a tank bioleaching process maintaining highly oxidative conditions is critical to enabling the dissolution of targeted minerals [5,6,10,11]. The main dissolution reactions are considered to take place between $Fe_2(SO_4)_3$ and sulphide minerals, followed by re-oxidation of the produced $FeSO_4$ by O_2 and acid, as shown in Equation (4) [12].

$$2FeSO_4 + 0.5O_2 + H_2SO_4 \rightarrow Fe_2(SO_4)_3 + H_2O \quad (4)$$

According to the above-mentioned Equations (1)–(4), high pyrrhotite content may cause several challenges in a tank bioleaching process. As pyrrhotite is highly reactive [8], it may deplete the system of oxidants and maintain non-oxidative conditions. This may take place due to the presence of pyrrhotite itself or due to its dissolution product H_2S that also consumes $Fe_2(SO_4)_3$ and O_2 [12]. Theoretically, this should result in halted leaching of targeted valuable minerals that require strongly oxidative conditions for their dissolution. Moreover, the non-oxidative conditions may lead to elevated acid consumption as pyrrhotite leaching proceeds via acid in these conditions [7]. Even though bioleaching microorganisms can produce H_2SO_4 from oxidising S^0, the realised net acid balance is easily negative when plenty of pyrrhotite is present. High acid consumption along with increased aeration may need to take place, especially in the first reactor of the bioleaching series, due to the high pyrrhotite reactivity and Fe oxidation–reduction cycle. Moreover, additional costs may be generated due to supplementing carbon for microorganisms as CO_2 since $CaCO_3$ cannot be utilised in acid-consuming processes.

The most common methods to separate pyrrhotite from ores are magnetic separation and flotation [1,2]. However, as these methods are not always viable, non-oxidative acid leaching has been considered to offer an alternative technique for removing pyrrhotite [13]. Similarly, as with magnetic separation and flotation, the non-oxidative acid leaching would result in benefits when applying the conventional pyrometallurgical recovery route, as decreased pyrrhotite content decreases slag and SO_2 production volume and transportation costs [14]. However, according to Equation (1), the non-oxidative acid leaching may also enable the recovery and valorisation of pyrrhotite-related Fe and S as $FeSO_4$ and H_2S, respectively [15]. Finally, the non-oxidative acid leaching may result in improved leaching kinetics and smaller chemical consumption in any later oxidative (bio)leaching of valuable metals, as explained earlier.

The non-oxidative acid leaching of pyrrhotite has been reported to start with an induction period, resulting in only minor H_2S and soluble Fe production. The induction period is followed by a rapid leaching phase with major H_2S and soluble Fe release. Finally, the dissolution is slowed down by passivation due to produced sulphur layers, which must be dissolved before continuing efficient pyrrhotite leaching [16]. The temperature and acidity have been observed to play a major role in leaching efficiency. According to the experiments conducted with HCl, at lower temperatures the non-oxidative leaching of pyrrhotite is slow and requires high acid concentration, while in higher temperatures the reaction is more active and proceeds to complete pyrrhotite dissolution with less acid [16,17]. When applying H_2SO_4 in non-oxidative leaching, an activation (e.g., with

hydrogen) may be required to decrease the Fe:S molar ratio of pyrrhotite closer to 1 to increase the dissolution efficiency [15]. Moreover, when using H_2SO_4, saturation may result in the formation of $FeSO_4$ precipitates. The increased H_2SO_4 concentration has been shown to decrease $FeSO_4$ solubility, while the temperature orders the number of hydrates of the crystal and influences the solubility [18].

In this study, an HS tailings sample, consisting of approximately 53 wt% pyrite and 24 wt% pyrrhotite, was subjected to non-oxidative H_2SO_4 leaching. The general objective was to utilise non-oxidative leaching as a pre-treatment before oxidative tank bioleaching for valuable metals (Co, Ni, Zn and Cu) recovery. The related tank bioleaching research will be reported later in an upcoming publication. The novelty of this research, compared to the existing literature, was to clarify the suitable operative process parameters of the non-oxidative leaching process. Therefore, a continuous mode validation test was conducted for the HS tailings sample to determine the H_2SO_4 consumption and retention time of the process. In addition, the possibilities of utilising the produced H_2S gas and $FeSO_4$ leachate was examined.

2. Materials and Methods

2.1. Sample Material, Milling and Analytics

The HS tailings sample was obtained from an active mill, where the milled input ore is treated via flotation to produce a Cu concentrate, a Zn concentrate and finally an HS tailings fraction that is stored in a pond. Two HS tailings sample barrels (namely HST-1 and HST-2) were obtained for the studies. Both HST-1 and HST-2 were first dried at room temperature and then homogenised by mixing. The additional milling of samples was conducted using a Mergan ball mill with stainless steel balls with full 5 kg loadings of the HS tailings for 200 min. The mill space and used water were purged with N_2 gas to prevent oxidation of sulphides during milling. Milling resulted in a d_{80} < 20 µm particle size according to a laser diffraction measurement (Beckman Coulter, Brea, CA, USA). The modal mineralogy of the sample was determined (MLA 600, built on Quanta 600 SEM by FEI Company and equipped with MLA software version 3.1.4.686, Thermo Fisher Scientific Inc., Waltham, MA, USA). The above-mentioned works were subcontracted from the Geological Survey of Finland (GTK). Milled HS tailings samples were packed under vacuum into bags and shipped to the VTT Technical Research Centre of Finland for leaching studies. The elemental composition was determined using ICP-OES (ICP-OES; 5100 SVDV, Agilent Technologies, Santa Clara, CA, USA) by complete digestion with microwave-assisted acid digestion (UltraWAVE, Milestone, Sorisole, Italy). In the actual leaching studies, pH and RedOx potential were measured using a Consort C3040 multiparameter analyser and Van London-pHoenix Co. pH and RedOx electrodes (Ag/AgCl in 3 M KCl; pH electrode calibration 1.68/4.01/7.00; RedOx electrode calibration +650 mV). Solution samples of leaching studies were analysed using ICP-OES (ICP-OES; 5100 SVDV, Agilent Technologies, Santa Clara, CA, USA).

2.2. Screening Tests

Screening tests of the non-oxidative leaching were conducted using a HST-1 sample. The leaching setup consisted of 1 L borosilicate glass reactor, equipped with a lid, baffles, an overhead stirrer and a blade impeller (1180 rpm). The temperature was controlled automatically with a heat plate and temperature sensor. The pH was controlled with an automatic titrator, using 4 M H_2SO_4 as a titrant. Released gases and fumes were collected from the reactor freeboard with a reflux condenser and transferred to two scrubbers (500 mL round-bottomed, two-neck borosilicate flasks) connected in series and both containing 350 mL of NaOH (400 g/L). The vacuum for gas collection was created with a water jet pump. As the reactors were not airtight, replacement air flowed into the reactor freeboard from the agitator shaft hole.

The non-oxidative leaching was conducted with 1 L working volume by first mixing distilled water and a dry HS tailings sample (200 g/L), heating the slurry and then starting

the acid titration. The desired pH (1.5 or 1.0) and temperature (25 °C or 80 °C) were then maintained for 300 min. During the operation, the acid consumption, pH, RedOx and temperature were monitored. Scrubber performance was monitored in the fume hood with an H_2S gas detector. Slurry samples (10 mL) were taken after 30, 120 and 300 min for leachate analysis and solids were returned to the reactor after 10 min of settling. After the tests, slurries were vacuum filtrated using a Buchner (filter pore size 0.45 µm) and the filtrate volume was measured. The leach residue was washed with distilled water (300 mL) in the Buchner. The leach residue was then removed from the filter and dried at 60 °C.

2.3. Validation Tests

The dry HS tailings sample (HST-2) was pulped with distilled water (200 g/L) at room temperature in a 10 L feed tank, equipped with a lid, baffles, an overhead stirrer and a blade impeller (800 rpm). The feed tank was refilled with 6 L of slurry every 90 min during continuous mode validation. The slurry was continuously pumped from the feed tank into the leaching circuit with a constant flowrate. The pH, RedOx, temperature, solid content, slurry volume and outflow of the feed tank were continually monitored.

The leaching circuit consisted of two 5 L stirred-tank reactors, equipped with lids, baffles, output nozzles, overhead stirrers and blade impellers (800 rpm). The temperature was controlled automatically with heat plates and temperature sensors. Reactors were connected in series as a cascade setup; the slurry was transported from the first leaching reactor (LR1) into the second leaching reactor (LR2), and from LR2 to the vacuum filtration Buchner using gravitational force via output nozzles. The leaching circuit was equipped with pumps to supplement 5.5 M H_2SO_4 primarily to LR1 and, if necessary, also to LR2. The molarity of acid solution was selected to compensate the evaporation. Both LR1 and LR2 were equipped with reflux condensers and formed gases were transferred to the scrubbing system. The scrubbing system consisted of two Duran GLS80 reaction vessels connected in series, both filled with 1 L NaOH (400 g/L), and suction was generated using a vacuum pump. As reactors were not airtight, replacement air flowed into the reactor airspace from the agitator shaft hole.

The leaching system was ramped up by filling LR1 and LR2 with slurry (200 g/L) and heating both reactors to 90 °C. Then, both reactors were supplemented with H_2SO_4 to reach and maintain pH 1.0 in batch mode for 60 min (half of the total retention time). After the ramp-up phase, the slurry feed pump was started (5.0 L/h) resulting in a continuous mode with a target hydraulic retention time (HRT) of 120 min. The continuous mode validation test was operated for 3 HRT cycles, which is generally considered to result in steady-state conditions if no changes are made to operational parameters. The target pH of the leach circuit was pH 1.0, measured from the LR2. The acid was provided with continuous and stable pumping (0.65 L/h) solely to LR1. The pH, Redox, temperature and acid flow were continually monitored during the operation. The solids content of LR1 and LR2 was determined on every half HRT cycle (60 min), while solution and solid analysis were conducted on every HRT cycle (120 min). LR2 output slurry flowrate was monitored to spot any anomalies during the operation. During the continuous mode validation test, filtration was conducted continuously for the LR2 output slurry. After removing the filtrate, leach residue was washed in the Buchner filter with distilled water (3000 mL), dried at room temperature, homogenised by mixing and analysed for mineralogical composition.

The validation test was performed in duplicate.

3. Results

3.1. Sample Characteristics

The elemental and mineralogical composition of HST-1 and HST-2 are presented in Tables 1 and 2, respectively. HST-1 was used for screening tests and HST-2 for continuous mode validation.

Table 1. Elemental composition of HST-1 and HST-2 sample batches.

	HST-1	HST-2
Element	**wt%**	**wt%**
Fe	37.1	40.3
S	35.5	38.6
Si	9.10	6.77
Ca	2.01	1.76
Mg	1.37	1.37
Zn	0.96	0.95
Co	0.75	0.79
Ni	0.30	0.38
Al	0.44	0.29
Cu	0.27	0.22
As	0.066	0.066
Na	0.060	0.048
Mn	0.024	0.019

Table 2. Mineralogical composition of HST-1 and HST-2 sample batches.

	HST-1	HST-2
Mineral	**wt%**	**wt%**
Pyrite	53.4	55.7
Pyrrhotite	24.4	23.3
Quartz	9.3	8.5
Tremolite	3.1	3.0
Sphalerite_Fe	1.7	1.3
Dolomite	1.4	2.0
Talc	1.1	0.3
Calcite	1.1	1.4
Biotite	0.7	0.1
Chalcopyrite	0.6	0.9
Plagioclase	0.6	0.7
Gypsum	0.4	0.1
Albite	0.4	0.1
Pentlandite_Co	0.3	0.6
Orthoclase	0.3	-
Apatite	0.2	0.1
Phlogopite	-	0.3
Pentlandite	-	0.2
Linnaeite_polydymite	-	0.1
Unknown	0.5	0.5
Total	100	100

The amount of pyrrhotite-related Fe was calculated using the mineralogical composition of $Fe_{0.875}S$ for pyrrhotite. The pyrrhotite-related Fe content was 14.7 wt% and 13.4 wt% in HST-1 and HST-2 samples, respectively. According to the mineralogical analysis (Table 2), the main readily acid-consuming minerals were pyrrhotite, dolomite and calcite [3]. The theoretical H_2SO_4 consumption of these minerals was calculated for HST-1 according to Equations (1), (5) and (6) for the non-oxidative leaching scenario. The resulting theoretical acid consumption was 299 kg 95% H_2SO_4 per one ton of tailings.

$$CaMg(CO_3)_2 + 2H_2SO_4 \rightarrow CaSO_4 + MgSO_4 + 2CO_2 + 2H_2O \quad (5)$$

$$CaCO_3 + H_2SO_4 \rightarrow CaSO_4 + CO_2 + H_2O \quad (6)$$

3.2. Screening Tests

In the screening tests, the pH (1.5 or 1.0) and temperature (25 °C or 80 °C) were maintained exactly at desired values without any anomalies. The H_2SO_4 consumption and RedOx are shown in Figure 1. The majority of the H_2SO_4 consumption was observed during the first 20 min in all tests, followed by minor consumption to maintain the operating pH. At 25 °C, the RedOx remained stable at +400 mV (pH 1.5) or +450 mV (pH 1.0), while at 80 °C it fell first to +250 mV and finally to 0 mV.

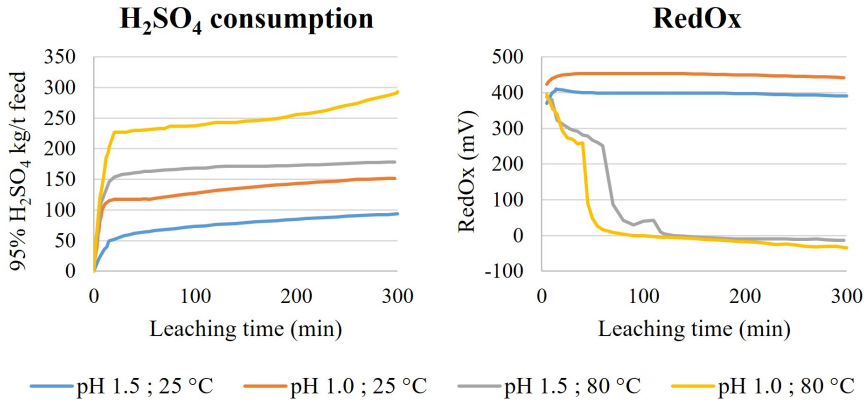

Figure 1. H_2SO_4 consumption (expressed as kg 95% H_2SO_4 per one ton of feed material) and RedOx in screening tests.

Fe, Zn, Cu, Co and Ni concentrations in solution during the leaching are shown in Figure 2. At 25 °C, Fe concentration increased slowly during the whole leaching time, while at 80 °C Fe concentration rose rapidly during the first 20 min. Later, at pH 1.0 and 80 °C, Fe concentration increased until the end of the experiment, while at pH 1.5 and 80 °C Fe concentration levelled. At 25 °C, Zn concentration increased throughout the experiment, while at 80 °C Zn concentration first increased rapidly, and then levelled. At both 25 °C and 80 °C, Cu, Co and Ni had a rapid increase in concentration during the first 20 min. Then, at 25 °C concentrations increased slowly, while at 80 °C concentrations started to decrease.

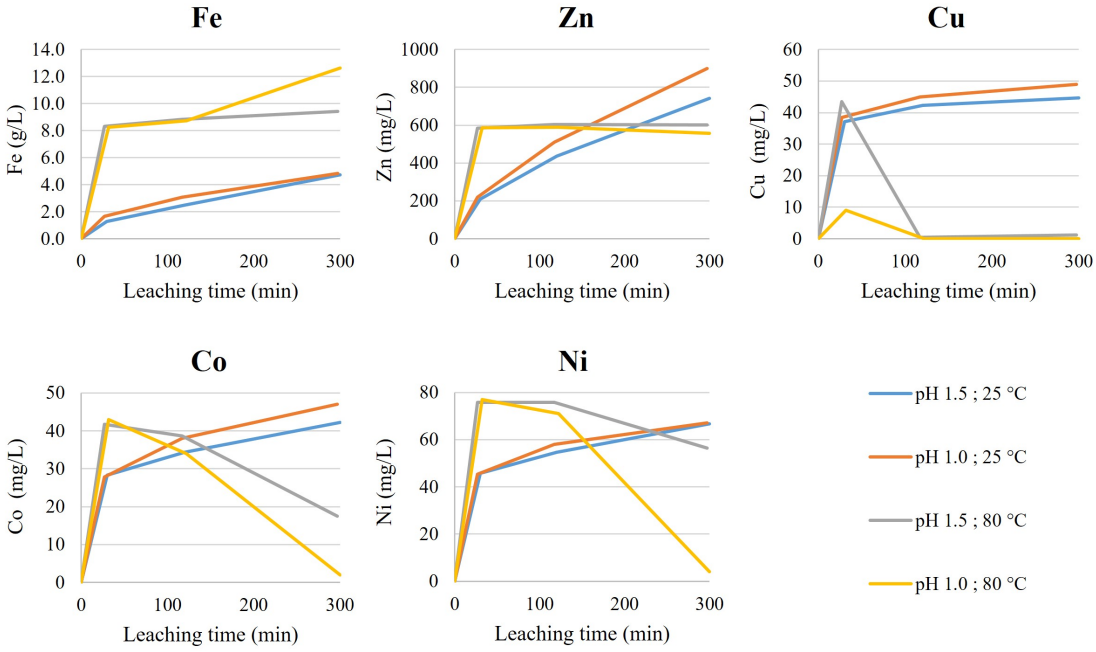

Figure 2. Concentrations of Fe, Zn, Cu, Co and Ni in solution during the leaching.

The final leaching yields of pyrrhotite (calculated according to the leaching of pyrrhotite-based Fe), Zn, Cu, Co and Ni at 80 °C tests are shown in Table 3.

Table 3. Calculated leaching yields of pyrrhotite, Zn, Cu, Co and Ni in tests conducted at 80 °C.

Test	Leaching Yield (%)				
	Pyrrhotite	Zn	Cu	Co	Ni
pH 1.5; 80 °C	51%	30%	0%	1%	9%
pH 1.0; 80 °C	58%	30%	0%	0%	1%

3.3. Continuous Mode Validation

During the continuous mode validation test, all H_2SO_4 was supplemented into the LR1; LR2 did not require any acid additions. The pH in LR1 and LR2 was 0.9 ± 0.1 and 1.0 ± 0.1, respectively. Temperature was maintained at 90 ± 2 °C. No technical challenges, such as pump blockages or flow disruptions, were encountered. Generally, the process was very stable and no adjustments were made during the operation. Foaming was minor, even though no foam-inhibitor equipment was installed. The acid solution used (5.5 M H_2SO_4) provided more water to the system than was consumed by evaporation. This resulted in an actual HRT of 106 min, instead of the planned 120 min (calculated according to the measured LR2 output volume flow). The total acid consumption of the process was 427 kg/t HS tailings (expressed as 95% H_2SO_4).

RedOx in Test 1 and Test 2 are shown in Figure 3. In both tests, RedOx was maintained at slightly negative during the whole operation. Generally, the RedOx in LR2s were slightly higher than in LR1s.

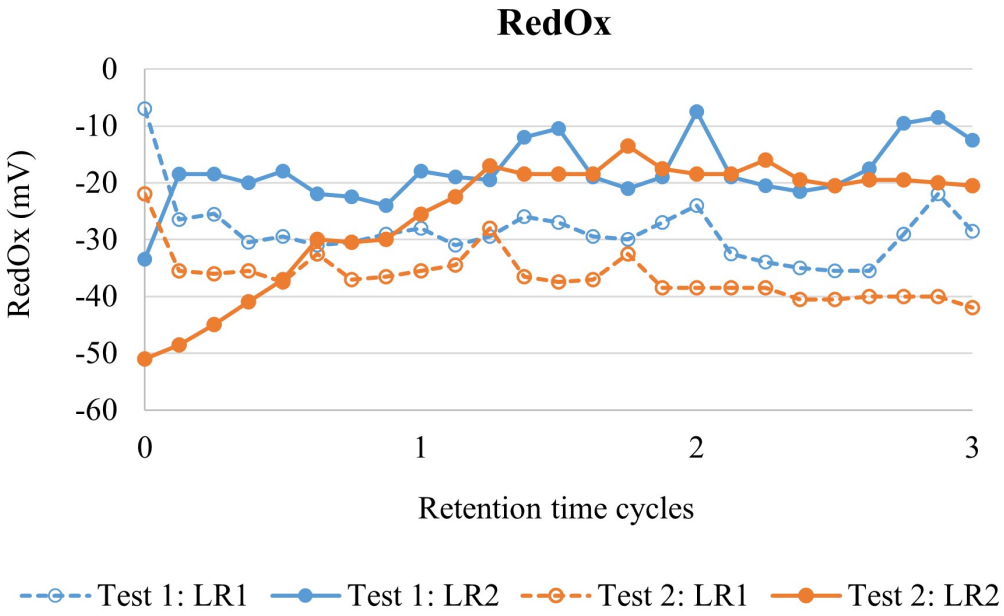

Figure 3. RedOx (mV) in the continuous mode tests. LR1 = the first leaching reactor, LR2 = the second leaching reactor.

Fe, Zn and Ni concentration during the continuous mode tests are presented in Figure 4. Fe and Zn concentrations stabilised during the operation after three retention time cycles 20–21 g/L and 240–270 mg/L in output solution (LR2), respectively. Ni concentration was very low in LR1 of both tests (28–29 mg/L) but increased in LR2 during the operation, with the final output solution having a concentration of 160–180 mg/L. The concentration of Cu and Co were <0.06 mg/L and <1.40 mg/L throughout the tests in every reactor. The averages of Ca, Mg, Al and Mn concentrations in the output solution were 720 mg/L, 680 mg/L, 160 mg/L and 40 mg/L, respectively.

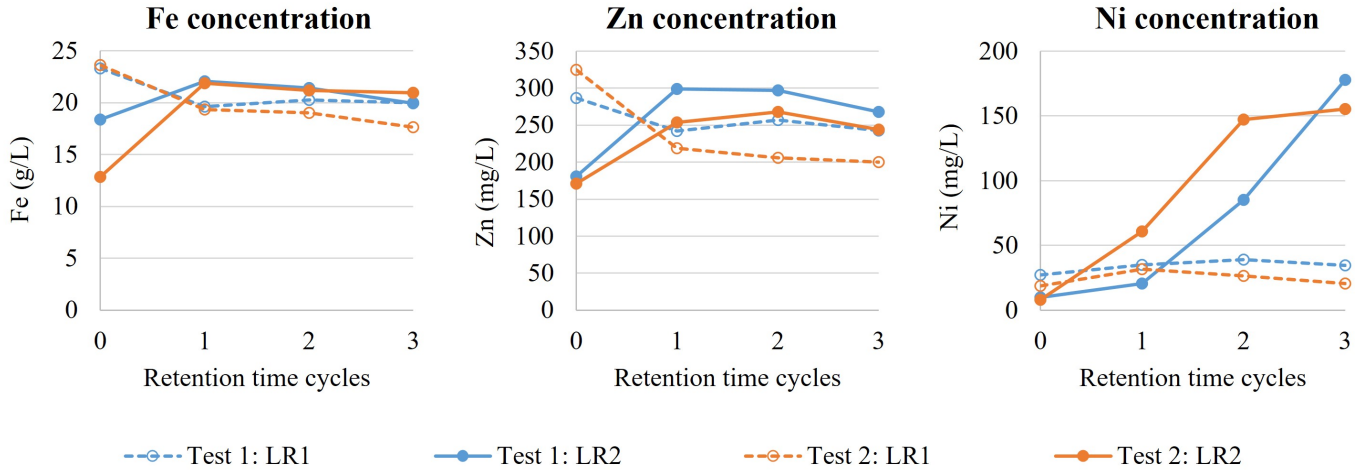

Figure 4. Concentration of Fe, Zn and Ni in continuous mode tests. LR1 = the first leaching reactor, LR2 = the second leaching reactor.

The leaching yields were determined after three retention time cycles for pyrrhotite (calculated according to the leaching of pyrrhotite-based Fe), Zn, Cu, Co and Ni (Table 4).

Table 4. Calculated leaching yields of pyrrhotite, Zn, Cu, Co and Ni after three retention time cycles in continuous mode tests.

Test	Leaching Yield (%)				
	Pyrrhotite	**Zn**	**Cu**	**Co**	**Ni**
Test 1 LR1	82%	13%	0%	0%	5%
Test 1 LR2	81%	14%	0%	0%	23%
Test 2 LR1	78%	11%	0%	0%	3%
Test 2 LR2	85%	13%	0%	0%	20%

The mineralogical composition of the solid leach residue is shown in Table 5. No pyrrhotite, talc or dolomite were detected in the leach residue. However, a major amount of $FeSO_4$ was found in the leach residues.

Table 5. Mineralogical composition of mixed solid leach residue (SLR).

Mineral	SLR (wt%)
Pyrite	64.3
Fe-sulphate	12.1
Quartz	7.8
Mixture of Fe-sulphate and quartz	3.6
Fe-Si-sulphate cement	1.8
Chalcopyrite	1.7
Sphalerite	1.6
Co-pentlandite	1.4
Tremolite	1.2
Mixture of goethite and gypsum	1.0
Pyrite inclusion in tremolite	0.7
Fe-sulphate alteration	0.6
Talc	0.4
Plagioclase	0.3
Gypsum	0.3
Unknown	0.4
Total	100

4. Discussion

4.1. Screening Tests

In the tests carried out at 25 °C, H_2SO_4 consumption (Figure 1) remained clearly lower than theoretical consumption. Moreover, RedOx (Figure 1) was relatively high, illustrating that no major H_2S generation was taking place. Therefore, non-oxidative pyrrhotite leaching, shown in Equation (1), did not occur. Previously, it has been reported that if temperature and acid concentration are too low, non-oxidative pyrrhotite leaching is not possible [16,17]. In the tests carried out at 80 °C the RedOx eventually collapsed, suggesting that pyrrhotite leaching was proceeding via a non-oxidative H_2S-producing route. However, only at pH 1.0 and 80 °C H_2SO_4 consumption reached the theoretical acid consumption level. Fe concentrations in solutions (Figure 2) were remarkably higher in the tests conducted at 80 °C, which confirmed that the high temperature had a major role in pyrrhotite leaching. By decreasing the pH to 1.0 at 80 °C, the highest Fe concentration was reached and the pyrrhotite leaching yield was 58% (Table 3). The $FeSO_4$ saturation was considered not to be a limiting factor for the Fe dissolution as the final Fe concentration was only 12.6 g/L. Theoretically, in these conditions, Fe^{2+} saturation is approximately 100 g/L [18].

Regarding the selectiveness of pyrrhotite leaching against Zn, Cu, Co and Ni leaching, temperature was seen to have a major role. At 25 °C, all valuable elements were partly dissolving, giving poor selectivity compared to the pyrrhotite leaching (Figure 2). At 80 °C, valuable elements were also dissolving during the first 30 min of tests (Figure 2). However, along with the collapse of RedOx, Zn concentration in solution levelled, and Cu, Co and Ni concentrations started to decrease. As the collapsed RedOx illustrated the formation of H_2S as a pyrrhotite dissolution product, Zn, Cu, Co and Ni were likely precipitating as sulphides [19]. The sulphide precipitation of different metal sulphates is a complex phenomenon. Cu is known to precipitate at a very low pH, already at low S^{2-} concentrations in solution [20]. Indeed, rapid and complete Cu removal from the solution at 80 °C was observed (Figure 2). Co and Ni were removed from the leachate more slowly; removal was nearly complete at pH 1.0 but incomplete at pH 1.5. This was the opposite to the general understanding of sulphide precipitation phenomena, where Co and Ni precipitation should benefit from the elevating pH [20], and Ni may not even precipitate at low pH if H_2S gas is supplemented without a continuous base addition to stabilise the pH [21]. However, it is noteworthy that the observations in [20,21] were related to the ambient temperature and that higher temperature promotes Ni precipitation [19]. Moreover, in our research H_2S was generated from non-oxidative pyrrhotite leaching, with the first dissolution product being S^{2-}, which then reacted to HS^- and eventually to H_2S gas [16]. Thus, the situation in our tests was remarkably different compared to the typical scenarios of sulphide precipitation, in which the limiting factor for precipitation to take place is poor dissolution of H_2S gas into the solution and then formation of S^{2-} [19–21]. In our tests, the lower pH promoted a higher generation of S^{2-} due to more efficient pyrrhotite dissolution, which was considered to cause more complete precipitation of Co and Ni. Unlike Cu, Co and Ni, Zn concentration levelled in solution along with RedOx collapse (Figures 1 and 2). It was considered that sphalerite (the source of Zn) was dissolving via a non-oxidative leaching route, but leaching was eventually halted and stability reached due to elevated H_2S formation, as explained in [22].

4.2. Continuous Mode Validation

The temperature in continuous mode validation was increased to 90 °C to further intensify the pyrrhotite leaching, while the pH was maintained at 1.0 (fluctuation of ±0.1 pH-units was due to providing acid via stable volume flow). The new operational parameters and conducting leaching in the continuous mode resulted in remarkably higher acid consumption compared to the batch test at 80 °C and pH 1.0 (427 kg/t vs. 293 kg/t). Therefore, the acid-consuming reactions were more intensive. As the dissolved Fe concentrations in LR1 and LR2 were similar, it was considered that the pyrrhotite leaching took place nearly completely in LR1 (Figure 4). This was supported by the lack of any acid consumption

in LR2. Calculations based on solution analyses showed an 81%–85% leaching yield for pyrrhotite (Figure 4), while no pyrrhotite was found in the mineralogical analyses of the residues (Table 5). The reason for this could be the entrapment of the leach solution in the filter cake during the filtration process. Solid–liquid separation and the following washing procedure was observed to be slow, inefficient and challenging. This was confirmed by the presence of $FeSO_4$ in the leach residues as shown in Table 5.

Dissolved Ni concentrations in both LR1s were low; however, the concentrations rose rapidly in LR2s (Figure 4). The reason for this behaviour could be due to the higher concentration of S^{2-} in LR1, where most of the pyrrhotite dissolution takes place, compared to LR2. This was also confirmed by higher redox potentials in LR2 in comparison with LR1 (Figure 3). To minimise unwanted Ni leaching, process retention time should be shortened to keep leaching conditions as reducing as possible. For example, if considering the pyrrhotite leaching already complete in LR1 and applying the respective retention time of 50–60 min for the total process, the Ni leaching yield could have been decreased from 13.5% to 3.6% (Table 4). It is noteworthy that an industrial non-oxidative leaching process does not require complete pyrrhotite removal. Thus, by leaving some minor part of pyrrhotite untouched, the process would automatically remain in strongly reducing conditions that prevent the major Ni leaching.

Unlike Ni leaching, Zn dissolution was already taking place at LR1, most likely due to non-oxidative sphalerite acid leaching. When comparing to the batch experiment, the unwanted Zn leaching was halved in continuous mode tests. This was most likely due to the intensified pyrrhotite leaching, generating more S^{2-} to the system and halting eventual sphalerite leaching [22]. The other valuable metals, namely Cu and Co, did not dissolve in the continuous mode tests.

4.3. Produced Outputs and Their Utilisation

The non-oxidative H_2SO_4 leaching of pyrrhotite produced three material streams, namely a residual solid, a leachate and a gas stream. After the treatment, the residual solid still contained a vast majority of the valuable metals, mainly as sulphides (Table 5), which require an additional oxidative leaching process, such as bioleaching.

The leachate stream was acidic and strongly dominated by $FeSO_4$ (Figure 4), with minor impurities of Ca, Mg, Zn, Ni, Al and Mn. An $FeSO_4 \cdot 7H_2O$ product could be prepared from the leachate using crystallisation utilising evaporation and cooling, similarly to spent pickling acids [18]. However, it was emphasised that the Fe concentration was clearly too low for these technologies and leachate should be circulated in a non-oxidative leaching process to obtain higher Fe concentrations. Regarding the impurities, Mg, Al and Mn concentration would increase in circulation, while Ca would remain stable due to $CaSO_4$ saturation. Some increase in Zn and Ni concentration may take place, due to the partial non-oxidative sphalerite and Ni-hosting pyrrhotite leaching (if present). Some additional purification would most likely be needed for obtaining a sellable $FeSO_4 \cdot 7H_2O$ product after circulation.

One possibility is to use the produced leachate as process water for the later bioleaching circuit of residual solid. Unfortunately, this results in less benefits as $FeSO_4$ would oxidise to $Fe_2(SO_4)_3$, which would eventually be precipitated and discharged into a waste pond. Thus, even the $FeSO_4 \cdot 7H_2O$ recovery would be non-profitable in the non-oxidative leaching circuit; however, it may still have a notable positive impact for the complete plant by transforming a significant part of the Fe to the product instead of waste.

The gas stream was strongly dominated by H_2S, with some CO_2 and water vapour impurities. The generated H_2S can be collected and utilised later to recover sellable CuS, ZnS and (CoNi)S products. The H_2S requirement for these products, calculated according to Equation (7) (where $MeSO_4$ illustrates +2 charged cations), is shown to be more than enough for production of CuS, ZnS and (CoNi)S (Table 6). The excess H_2S is preferably recovered and sold as some S-product to the market. For example, the H_2S-containing gas stream could be fed to the Claus process for production of elemental S [15].

$$MeSO_4 + H_2S \rightarrow MeS + H_2SO_4 \quad (7)$$

Table 6. H_2S production and consumption balance in the plant utilising non-oxidative leaching of pyrrhotite, oxidative leaching of the residual solid and H_2S precipitation of CoNiS, ZnS and CuS from PLS.

Action	Explanation	H_2S kg/t Tailings
Non-oxidative leaching	100% conversion of pyrrhotite to H_2S.	+81.6
Precipitation of CoS	1.2x excess consumption of H_2S in precipitation.	5.5
Precipitation of NiS	1.2x excess consumption of H_2S in precipitation.	2.6
Precipitation of ZnS	1.2x excess consumption of H_2S in precipitation.	5.9
Precipitation of CuS	1.0x excess consumption of H_2S in precipitation.	1.2
Balance		+66.4

5. Conclusions

Pyrrhotite was removed via non-oxidative H_2SO_4 leaching from the high-sulphur tailings. By applying a high temperature (90 °C) and pH 1.0, the process resulted in a complete dissolution of pyrrhotite in a less than 120 min retention time, by consuming 427 kg of 95% H_2SO_4 per ton of feed material. The selectivity of the process was only moderate, as 13.5% and 21.5% of Zn and Ni were dissolved, respectively. The continuous mode tests indicated that by decreasing the retention time, Ni dissolution, in particular, can be minimised. The residual solid contained a vast majority of valuable metals and was a suitable feed for bioleaching. The non-oxidative pyrrhotite leaching produced an excess of H_2S that would be required for the precipitation of metal sulphides in downstream processing. The non-oxidative pyrrhotite leaching also resulted in an $FeSO_4$-dominated leachate that can be utilised for recovery. However, this was expected to require leachate circulation to increase Fe concentration and some impurities in the removal processes.

Author Contributions: Conceptualisation, J.M., V.M., M.K. and J.-E.S.; methodology, J.M., G.P. and V.M.; validation, J.M. and G.P.; formal analysis, J.M.; investigation, J.M., G.P. and M.K.; resources, M.K.; writing—original draft preparation, J.M. and G.P.; writing—review and editing, V.M., M.K., J.-E.S. and P.K.; visualisation, J.M.; supervision, V.M., M.K. and P.K. All authors have read and agreed to the published version of the manuscript.

Funding: This research was funded by the European Commission Horizon 2020 project NEMO "Nearzero-waste recycling of low-grade sulfidic mining waste for critical-metal, mineral and construction raw-material production in a circular economy" [Grant Agreement number 776846], https://h2020-nemo.eu/ (accessed on 5 December 2022).

Conflicts of Interest: The authors declare no conflict of interest.

References

1. Fuerstenau, M.C.; Chander, S.; Woods, P. Sulfide mineral flotation. In *Froth Flotation: A Century of Innovation*; Fuerstenau, M.C., Jameson, G.J., Yoon, R.H., Eds.; Society for Mining, Metallurgy and Exploration Inc.: Littleton, CO, USA, 2007; pp. 425–465.
2. Wills, B.A.; Finch, J.A. *Wills' Mineral Processing Technology: An Introduction to the Practical Aspects of Ore Treatment and Mineral Recovery*, 8th ed.; Elsevier Science & Technology: Oxford, UK, 2015.
3. Lottermoser, B.G. *Mine Wastes, Characterization, Treatment and Environmental Impacts*, 3rd ed.; Springer-Verlag: Berlin/Heidelberg, Germany, 2010.
4. Lindsay, M.B.J.; Moncur, M.C.; Bain, J.G.; Jambor, J.L.; Ptacek, C.J.; Blowes, D.W. Geochemical and mineralogical aspects of sulfide mine tailings. *Appl. Geochem.* **2015**, *57*, 157–177. [CrossRef]
5. Morin, D.H.R.; D'hugues, P. Bioleaching of a Cobalt-Containing Pyrite in Stirred Reactors. In *Biomining*; Rawlings, D.E., Johnson, D.B., Eds.; Springer: Berlin/Heidelberg, Germany, 2007.
6. Neale, J.; Seppälä, J.; Laukka, A.; Van Aswegen, P.; Barnett, S.; Gericke, M. The MONDO Minerals Nickel Sulfide Bioleach Project: From Test Work to Early Plant Operation. *Solid State Phenom.* **2017**, *262*, 28–32. [CrossRef]

7. Belize, N.; Yu-Wei, C.; Cai, M.-F.; Li, Y. A review of pyrrhotite oxidation. *J. Geochem. Explor.* **2004**, *84*, 65–76. [CrossRef]
8. Arpalahti, A.; Lundström, M. The leaching behavior of minerals from a pyrrhotite-rich pentlandite ore during heap leaching. *Miner. Eng.* **2018**, *119*, 116–125. [CrossRef]
9. Altinkaya, P.; Mäkinen, J.; Kinnunen, P.; Kolehmainen, E.; Haapalainen, M.; Lundström, M. Effect of biological pretreatment on metal extraction from flotation tailings for chloride leaching. *Miner. Eng.* **2018**, *129*, 47–53. [CrossRef]
10. Mäkinen, J.; Heikola, T.; Salo, M.; Kinnunen, P. The Effects of Milling and pH on Co, Ni, Zn, and Cu Bioleaching from Polymetallic Sulfide Concentrate. *Minerals* **2021**, *11*, 317. [CrossRef]
11. Mäkinen, J.; Salo, M.; Khoshkhoo, M.; Sundkvist, J.-E.; Kinnunen, P. Bioleaching of cobalt from sulfide mining tailings; a mini-pilot study. *Hydrometallurgy* **2020**, *19*, 105418. [CrossRef]
12. Sand, W.; Gehrke, T.; Jozsa, P.-G.; Schippers, A. (Bio)chemistry of bacterial leaching—Direct vs. indirect bioleaching. *Hydrometallurgy* **2001**, *59*, 159–175. [CrossRef]
13. Abrahamsson, F. Leaching of Pyrrhotite from Nickel Concentrate. Master's Thesis, Luleå University of Technology, Luleå, Sweden, 2017.
14. Peek, E.; Barnes, A.; Tuzun, A. Nickeliferous pyrrhotite-waste or a resource? *Miner. Eng.* **2011**, *24*, 625–637. [CrossRef]
15. Subramanian, K.; Stratigakos, E.; Jennings, P. Hydrometallurgical processing of pyrrhotite. *Can. Metall. Q.* **1972**, *11*, 425–434. [CrossRef]
16. Thomas, J.E.; Jones, C.F.; Skinner, W.M.; Smart, R.S. The role of surface sulfur species in the inhibition of pyrrhotite dissolution in acid conditions. *Geochim. Cosmochim. Acta* **1998**, *62*, 1555–1565. [CrossRef]
17. Ingraham, T.; Parsons, H.; Cabri, L. Leaching of pyrrhotite with hydrochloric acid. *Can. Metall. Q.* **1972**, *11*, 407–411. [CrossRef]
18. Seyeler, J.K.; Thornton, W.E.; Householder, M.K.H. *Sulfuric Acid and Ferrous Sulfate Recovery From Waste Pickle Liquor*; US Government Printing Office: Washington, DC, USA, 1974.
19. Lewis, A.E. Review of metal sulphide precipitation. *Hydrometallurgy* **2010**, *104*, 222–234. [CrossRef]
20. Monhemius, J. Precipitation diagrams for metal hydroxides, sulfides, arsenates and phosphates. *Tran. Inst. Min. Metall. Sect. C* **1977**, *86*, 202–206.
21. Karbanee, N.; van Hille, R.P.; Lewis, A.E. Controlled Nickel Sulfide Precipitation Using Gaseous Hydrogen Sulfide. *Ind. Eng. Chem. Res.* **2008**, *47*, 1596–1602. [CrossRef]
22. Crundwell, F.K.; Verbaan, B. Kinetics and Mechanisms of the Non-oxidative Dissolution of Sphalerite (Zinc Sulphide). *Hydrometallurgy* **1987**, *17*, 369–384. [CrossRef]